Asress Mulugeta Biadgo

Addis Ababa University
Technology Faculty
Department of Mechanical Engineering

Aleksandar Simonovic

University of Belgrade
Faculty of Mechanical Engineering

Dragan Komarov

University of Belgrade
Faculty of Mechanical Engineering

Slobodan Stupar

University of Belgrade
Faculty of Mechanical Engineering

Numerical and Analytical Investigation of Vertical Axis Wind Turbine

The majority of wind turbine research is focused on accurately efficiency prediction. This work highlights the progress made in the development of aerodynamic models for studying Vertical-Axis Wind Turbines (VAWTs) with particular emphasis on streamtube approach. Numerical and analytical investigation is conducted on straight blade fixed pitch VAWT using NACA0012 airfoil as a blade profile to assess its performance. Numerical simulation is done for two-dimensional unsteady flow around the same VAWT model using ANSYS FLUENT by solving Reynolds-averaged Navier-Stokes equations. Finally, comparison of the analytical results using double multiple streamtube (DMST) model with computational fluid dynamics (CFD) simulation has been done. Both the CFD and DMST results have shown minimum and/or negative torque and performance at lower tip speed ratios for the modeled turbine, which implies the inability of NACA0012 to self start.

Keywords: Vertcial Axis Wind Turbine, Airfoil, Momentum Model, CFD

1. INTRODUCTION

There are two categories of modern wind turbines, namely Horizontal Axis Wind Turbines (HAWTs) and Vertical Axis Wind Turbines (VAWTs), which are used mainly for electricity generation. Though VAWTs have inherent advantages, HAWTs are dominant commercially. The principal advantages of the vertical axis forms are their ability to accept wind from any direction without yawing. The absence of yaw system requirement simplifies the design of the turbine. Blades of VAWT may be of uniform section and untwisted, making them relatively easy to fabricate or extrude, unlike the blades of HAWT, which should be twisted and tapered for optimum performance. Furthermore, almost all of the components requiring maintenance are located at ground level facilitating the maintenance work appreciably. However, its high torque fluctuations with each revolution, no self starting capability are the drawbacks [1,2].

VAWTs had received little attention until the oil crises of the early 1970s. The oil crises stimulated a revival of interest in a range of renewable energy conversion devices including drag and lift type (Savonius and Darrieus) of VAWT. Then interest in VAWT has declined since 1980s as the propeller shaped HAWT has become established as the standard form of wind turbine. Recently Darrieus type VAWT is attracting many researchers for its inherent advantages and diversified applications. Several comparative advantage studies show that VAWTs are advantageous to HAWTs in several aspects especially if the inability of the turbine to self start is resolved. As the vertical axis wind turbine has a rotational axis perpendicular to the oncoming airflow, the aerodynamics involved is more complicated than of the more conventional HAWT [3].

Many wind turbine researches are focused on accurately predicting efficiency. Various computational models exist, each with their own strengths and weaknesses that attempt to accurately predict the performance of a wind turbine. Being able to numerically predict wind turbine performance offers a possibility to reduce the number of experimental tests that are needed, with the major benefit being that computational studies are more economical than costly experiments.

The design of VAWT blades, to achieve satisfactory level of performance; starts with knowledge of the aerodynamic forces acting on the blades. In this article, VAWT blade design from the aspect of aerodynamics is investigated.

The structural design of VAWT blades is also as important as their aerodynamic design. The dynamic structural loads which a rotor will experience play the major role in determining the lifetime of the rotor. Obviously, aerodynamic loads are a major source of dynamic structural behaviour, and ought to be accurately determined. In addition, the blade geometry parameters are required for dynamic load analysis of wind turbine rotors.

2. AERODYNAMICS OF VAWT

Wind turbine power production depends on the interaction between the rotor and the wind. Many factors play a role in the design of a wind turbine rotor, including aerodynamics, generator characteristics, blade strength and rigidity, noise levels, etc. But since a wind energy conversion system is largely dependent on maximizing its energy extraction, rotor aerodynamics play important role in the minimization of the cost of energy.

2.1 The Actuator Disk Theory and The Betz Limit

A simple model, generally attributed to Betz (1926) can be used to determine the power, the thrust of the wind on the ideal rotor and the effect of the rotor operation on the local wind field. The simplest aerodynamic model of a wind turbine is known as 'actuator disk model' in which the rotor is assumed as a homogenous disk that extracts energy from the wind.

The theory of the ideal actuator disk is based on the following assumptions[4]:

- Homogenous, incompressible, steady state fluid flow, no frictional drag;
- The pressure increment or thrust per unit area is constant over the disk;
- The rotational component of the velocity in the slipstream is zero;
- There is continuity of velocity through the disk;
- An infinite number of blades.

The analysis of the actuator disk theory assumes a control volume as shown in Figure 1.
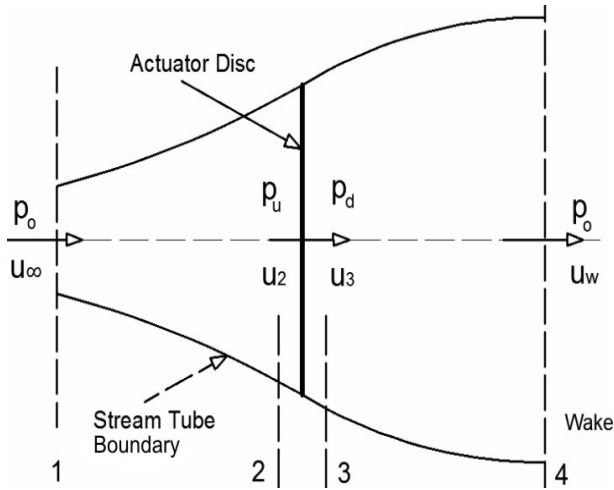
Figure 1. Idealized flow through a wind turbine represented by a non-rotating actuator disk.

In the above control volume, the only flow is across the ends of the stream tube. The turbine is represented by a uniform actuator disk which creates a discontinuity of pressure in the stream tube of air flowing through it. Note also that this analysis is not limited to any particular type of wind turbine.

From the assumption that the continuity of velocity through the disk exists, the velocities at section 2 and 3 are equal to the velocity at the rotor:

$$u_2 = u_3 = u_R \qquad (1)$$

For steady state flow, air mass flow rate through the disk can be written as:

$$\dot{m} = \rho A u_R \qquad (2)$$

Applying the conservation law of linear momentum to the control volume enclosing the whole system, the net force can be found on the contents of the control volume. That force is equal and opposite to the thrust, T which is the force of the wind on the wind turbine. Hence, from the conservation of linear momentum for a one-dimensional, incompressible, steady flow the thrust is equal and opposite to the change in momentum of air stream:

$$T = -\dot{m}(u_\infty - u_w) \qquad (3)$$

Work is not done on either side of the wind turbine rotor. Thus the Bernoulli equation can be used in the two control volumes on either side of the actuator disk. Between the free-stream and upwind side of the rotor (from section 1 to 2 in Figure 1) and between the downwind side of the rotor and far wake (from section 3 to 4 in Figure 1) respectively:

$$p_o + \frac{1}{2}\rho u_\infty{}^2 = p_u + \frac{1}{2}\rho u_R{}^2 \qquad (4)$$

$$p_d + \frac{1}{2}\rho u_R{}^2 = p_o + \frac{1}{2}\rho u_w{}^2 \qquad (5)$$

The thrust can also be expressed as the net sum forces on each side of the actuator disk:

$$T = Ap' \qquad (6)$$

where,

$$p' = (p_u - p_d) \qquad (7)$$

By using Equations (4) and (5), the pressure decrease, p' can be found as:

$$p' = \frac{1}{2}\rho(u_\infty{}^2 - u_w{}^2) \qquad (8)$$

And by substituting Equation (8) in to Equation (6):

$$T = \frac{1}{2}\rho A(u_\infty{}^2 - u_w{}^2) \qquad (9)$$

By equating the thrust values from Equation (3) in which substituting Equation (2) in place of $\dot{m}$ and Equation (9), the velocity at the rotor plane can be found as:

$$u_R = \frac{u_\infty + u_w}{2} \qquad (10)$$

If an axial induction factor, a is defined as the fractional decrease in the wind velocity between the free stream and the rotor plane, then

$$a = \frac{u_\infty - u_R}{u_\infty} \qquad (11)$$

$$u_R = u_\infty(1 - a) \qquad (12)$$

Using Equation (10) and (12) one can get:

$$u_w = u_\infty(1 - 2a) \qquad (13)$$

The velocity and pressure distribution are illustrated in Figure 2. Because of continuity, the diameter of flow field must increase as its velocity decreases and there occurs sudden pressure drop at rotor plane which contributes to the torque of rotating turbine blades.

The power output, P is equal to the thrust times the velocity at the rotor plane:
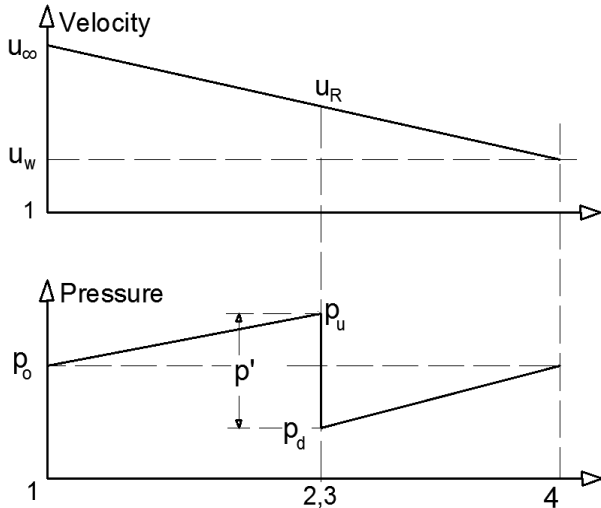
$$P = Tu_R \quad (14)$$

Figure 2. Velocity and pressure distribution along the stream tube

Using Equation (9),

$$P = \frac{1}{2}\rho A(u_\infty{}^2 - u_w{}^2)u_R \quad (15)$$

and substituting for u_R and u_w from Equations (12) and (13) to Equations (15):

$$P = 2\rho A a (1-a)^2 u_\infty{}^3 \quad (16)$$

The power performance parameters of a wind turbine can be expressed in dimensionless form, in which the power coefficient, C_P is given in the following equation:

$$C_P = \frac{P}{0.5\rho u_\infty{}^3 A} \quad (17)$$

Using Equation (16) and (17), the power coefficient C_P becomes:

$$C_P = 4a(1-a)^2 \quad (18)$$

The maximum CP is determined by taking the derivative of Equation (18) with respect to a and setting it equal to zero which yields:

$$(C_P)_{max} = \frac{16}{27} = 0.5926 \quad (19)$$

when, $a = 1/3$.

This result indicates that if an ideal rotor were designed and operated so that the wind speed at the rotor were 2/3 of the free stream wind speed, then it would be operating at the point of maximum power production. This is known as the Betz limit.

From Equations (9), and (13) the axial thrust on the disk can be written in the following form:

$$T = 2\rho A a (1-a)u_\infty{}^2 \quad (20)$$

Similar to the power coefficient, thrust coefficient can be defined by the ratio of thrust force to dynamic pressure as shown in the following equation:

$$C_T = \frac{T}{0.5\rho u_\infty{}^2 A} \quad (21)$$

Using Equation (20) and (21), the thrust coefficient C_T becomes:

$$C_T = 4a(1-a) \quad (22)$$

Note that C_T has a maximum of 1.0 when $a = 0.5$ and the downstream velocity is zero. At maximum power output ($a = 1/3$), C_T has a value of 8/9.

2.2 Aerodynamics of Straight Blade Darrieus Type VAWT

As the VAWT have a rotational axis perpendicular to the oncoming airflow, the aerodynamics involved are more complicated than of the more conventional HAWT. The main disadvantages of VAWT are the high local angles of attack involved and the wake coming from the blades in the upwind part and from the axis.

Compared to Savonius rotor, Darrieus rotor usually works at relatively high tip speed ratio which makes it attractive for wind electric generators. However, they are not self-starting and require external 'excitation' to cut-in [1, 2].
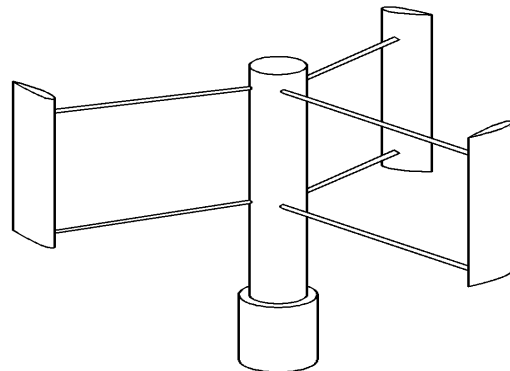
Figure 3. Straight blade Darrieus type VAWT

If the straight blade Darrieus type VAWT is represented in a two dimensional way (Figure 4) the aerodynamic characteristics are more obvious.
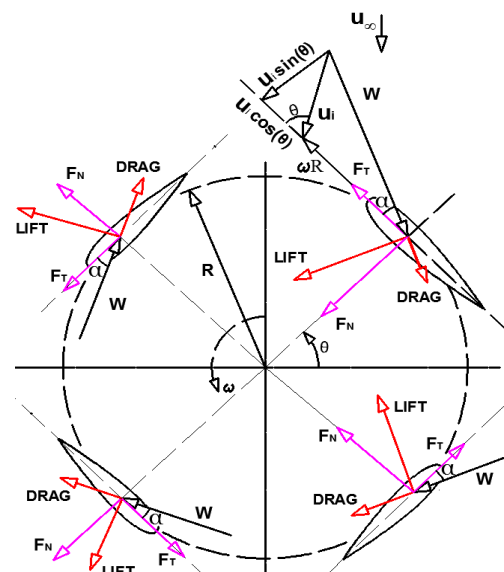
Figure 4. VAWT flow velocities and blade

As can be seen from the Figure 4 the relative velocity, w can be obtained from the cordial velocity component and normal velocity component:

$$w = \sqrt{(u_i \sin(\theta))^2 + (u_i \cos(\theta) + \omega R)^2} \quad (23)$$

where u_i is the induced velocity through the rotor, ω is the rotational velocity, R is the radius of the turbine, and θ is the azimuth angle.

The relative velocity can be written in non-dimensional form using free stream velocity:

$$\frac{w}{u_\infty} = \sqrt{(\frac{u_i}{u_\infty} \sin(\theta))^2 + (\frac{u_i}{u_\infty} \cos(\theta) + \frac{\omega R}{u_\infty})^2} \quad (24)$$

From Equation (12) substituting the induced velocity u_i in place of u_R results:

$$u_i = u_\infty (1-a) \quad (25)$$

Since $\omega R / u_\infty = \lambda$ and using Equation (25), Equation (24) can be rewritten as:

$$\frac{w}{u_\infty} = \sqrt{((1-a)\sin\theta)^2 + ((1-a)\cos\theta + \lambda)^2} \quad (26)$$

From the geometry of Figure 4, the local angle of attack can be expressed as:

$$\tan(\alpha) = \frac{u_i \sin(\theta)}{u_i \cos(\theta) + \omega R} \quad (27)$$

Similarly to relative velocity the induced velocity can be put in non-dimensional form and using Equation (25) the above equation yields:

$$\alpha = \tan^{-1}\left(\frac{(1-a)\sin(\theta)}{(1-a)\cos(\theta) + \lambda}\right) \quad (28)$$

The normal and tangetial force coefficients can be expressed as:

$$C_n = C_L \cos(\alpha) + C_D \sin(\alpha) \quad (29)$$

$$C_t = C_L \sin(\alpha) - C_D \cos(\alpha) \quad (30)$$

where C_L is the lift coefficient and C_D is the drag coefficient for angle of attack α.

Then the normal and tangential forces for single blade at a single azimuthal location are:

$$F_N = \frac{1}{2}\rho w^2 (hc) C_n \quad (31)$$

$$F_T = \frac{1}{2}\rho w^2 (hc) C_t \quad (32)$$

where 'h' is the blade height and 'c' is the blade chord length.

Using Figure 4, the instantaneous thrust force which is the force of the wind on the turbine experienced by one blade element in the direction of the airflow, is:

$$T_i = F_T \cos\theta - F_N \sin\theta \quad (33)$$

Using Equation (29), (30), (31) (32) and (33) the instantaneous thrust force can be expressed as:

$$T_i = \frac{1}{2}\rho w^2 (hc)(C_n \sin\theta - C_t \cos\theta) \quad (34)$$

Since it is tangential force component that drives the rotation of the wind turbine and produces the torque necessary to generate electricity the instantaneous torque or the torque by a single blade at a single azimuthal location is:

$$Q_i = F_T R \quad (35)$$

Substituting Equation (32) in Equation (35) yields:

$$Q_i = \frac{1}{2}\rho w^2 (hc) C_t R \quad (36)$$

2.2 Computational Modelling of VAWT

Various computational models exist, each with their own strengths and weaknesses that attempt to accurately predict the performance of a wind turbine. A survey of aerodynamic models used for the prediction of VAWT performance was conducted by Islam [3] and Paraschivoiu [5, 6]. The three major models include momentum models, vortex model, and computational fluid dynamics (CFD).

This work particularly emphasizes the momentum models to predict the performance of Darrieus type VAWT using double multiple streamtube model as well as computational fluid dynamics method.

Momentum based models are based on the actuator disk theory, which is generally used for rotor aerodynamics, adjusted for the VAWT. The basic model is called the single streamtube model. This model was developed in two directions (Figure 5).
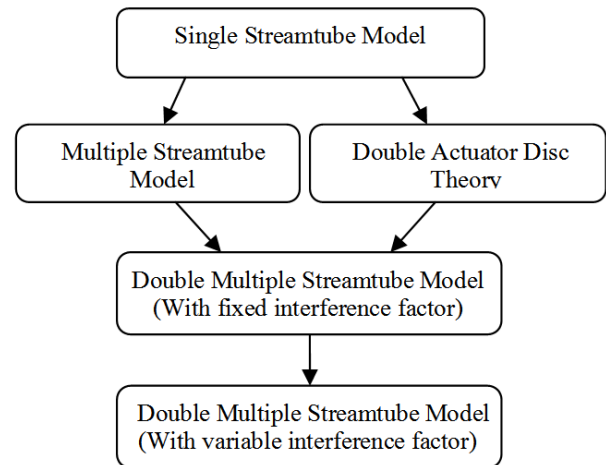

Figure 5. Overview of the development of the streamtube models

2.2.1 Single Streamtube Model

This model was first developed by Templin for the VAWT [7]. It is based on the actuator disk theories applicable for propellers as discussed above in section

2.1 and is the most basic model based on the momentum theory. The flow through the turbine is assumed to have one constant velocity.

2.2.2 Multiple Streamtube Model

Multiple streamtube model is developed by Strickland [8] and is also based on the momentum theory. The main improvement with respect to the single streamtube model is that more streamtubes make different induced velocities possible (Figure 6). Each stream tube has its own velocity, allowing a change in velocity depending on the direction perpendicular to the free stream flow. The accuracy is dependent on the number of streamtubes used. The momentum balance is carried out separately for each stream tube.

For each of these streamtubes the momentum equations and blade elements have to be calculated, resulting in *"N"* interference (induction) factors.

The total span of the single streamtube is divided in multiple stream tubes using a fixed angle $\Delta\theta$:

$$\Delta\theta = \frac{2\pi}{N_\theta} \tag{37}$$

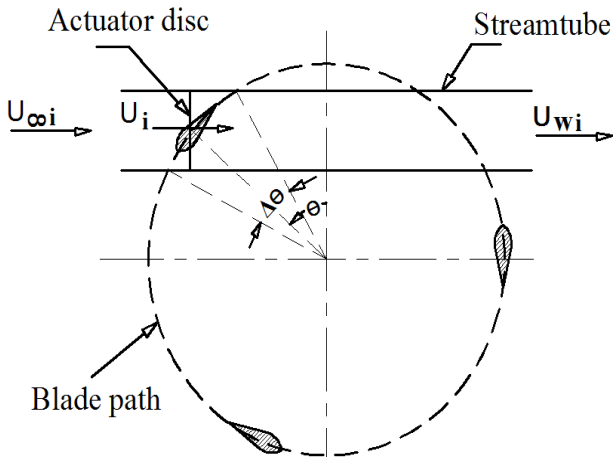Here, a single blade passes each streamtube twice per revolution in the upstream and downsteam.

Figure 6. 2D Schematic of the streamtube Model

The instantaneous thrust on a single blade at one azimuthal location is given in Equation (34). The average aerodynamic thrust with *"B"* number of blades and noting that each of *"B"* blade elements spend $\Delta\theta/\pi$ percent of their time in the streamtube, thus:

$$T_{avg} = 2(\frac{B\Delta\theta}{\pi}T_i) \tag{38}$$

Considering swept area of the turbine for single streamtube $A = hR\Delta\theta\sin\theta$, one can easily get the non dimensional thrust coefficient as:

$$C_T = \frac{T_{avg}}{0.5\rho u_\infty^2 (hR\Delta\theta\sin\theta)}$$

$$= \left(\frac{Bc}{2R}\right)\left(\frac{w}{u_\infty}\right)^2 \frac{2}{\pi}\left(C_t\frac{\cos\theta}{\sin\theta} - C_n\right) \tag{39}$$

The instantaneous torque by single blade is given by Equation (36). Then the average torque on rotor by *"B"* number of blades on the complete interval $(0 < \theta < 2\pi)$ and blade length *"h"* is given by:

$$Q_{avg} = B \times \sum_{i=1}^{N_\theta} \frac{\left[\frac{1}{2}\rho w^2 (hc)C_t * R\right]}{N_\theta} \tag{40}$$

The torque coefficient can be defined as:

$$C_Q = \frac{Q_{avg}}{0.5\rho u_\infty^2 (Dh)R} \tag{41}$$

$$C_Q = \left(\frac{Bc}{D}\right)\sum_{i=1}^{N_\theta} \frac{\left(\frac{w}{u_\infty}\right)^2 C_t}{N_\theta} \tag{42}$$

$$C_P = C_Q\lambda \tag{43}$$

2.2.3 Double Actuator Disk Theory

The main disadvantage of the previous model is the inability to make a distinction between the upwind and downwind part of the turbine. To make this possible, two actuator disks are placed behind each other, connected at the center of the turbine (Figure 7).

In a similar way, as discussed in section 2.1, in this model, for the two actuator disks, velocities are determined by two interference factors, a and a'. The induced velocity on the upstream will be the average of the air velocity at far upstream and the air velocity at downstream equilibrium. Thus the induced velocity for the first actuator disk can be written as:

$$u_i = \frac{u_\infty + u_e}{2} \tag{44}$$

$$u_i = (1-a)u_\infty \tag{45}$$

where u_i is the induced velocity in upwind part of the turbine or the uniform wind velocity at the rotor plane in the first actuator disk and u_e is the air velocity at the downstream equilibrium.
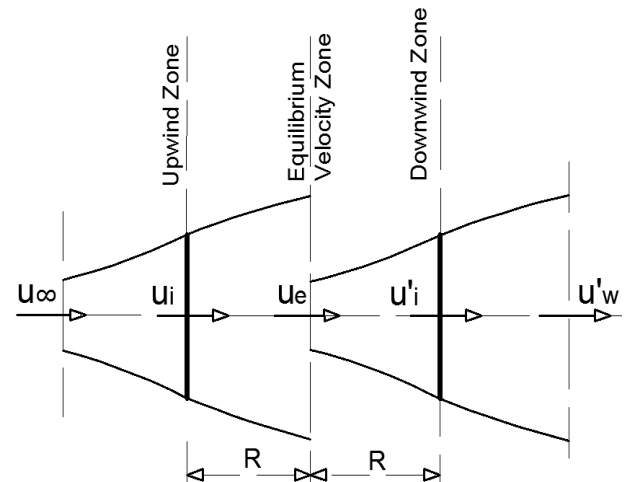

Figure 7. Schematic of the two actuator disk behind each other

Using Equation (44) and (45) the air velocity at the downstream equilibrium can be expressed as:

$$u_e = (2u_i - u_\infty) = (1-2a)u_\infty \qquad (46)$$

Similarly for the second actuator disk, the induced velocity and induction factor in the downwind part of the turbine can be stated as:

$$u_i' = \frac{u_e + u_w'}{2} \qquad (47)$$

$$a' = \frac{u_e - u_i'}{u_e} \qquad (48)$$

Using Equation (46) and (48), the induced velocity in the downwind part of the turbine becomes:

$$u_i' = (1-a')(1-2a)u_\infty \qquad (49)$$

where, $u_i^{'}$ is the induced velocity in the downwind zone and a' is the induction (interference) factor in the downwind zone.

2.2.4 Double Multiple Streamtube Model (DMST)

The double multiple streamtube model described by Loth and McCoy, 1983 and Paraschivoiu and Delclaux, 1983 combines the multiple stream tubes model with the double actuator disk theory. It allows to model velocity variations in the direction perpendicular to the free stream flow and between the upwind and downwind part of the turbine. The previous models were not able to calculate the influence of the upwind part on the downwind part. It is easily understood that the wind velocities at the upwind part are larger than these at the downwind part, because the blades have already extracted energy from the wind.

The turbine's interaction with the wind in the upwind and downwind passes of the blades is treated separately. The assumption is made that the wake from the upwind pass is fully expanded and the ultimate wake velocity has been reached before the interaction with the blades in the downwind pass. The downwind blades therefore see a reduced 'free-stream' velocity. This approach more accurately represents the variation in flow through the wind turbine.
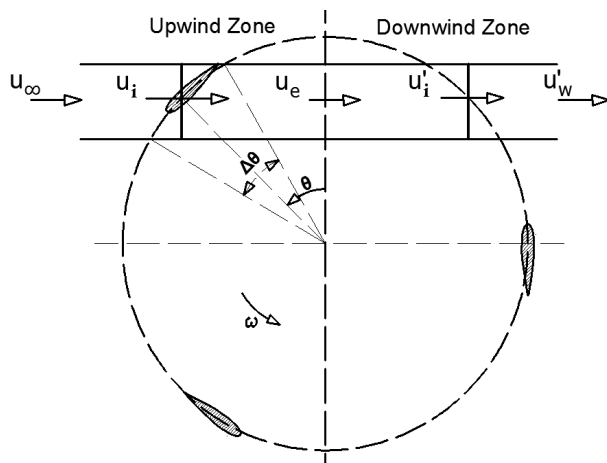

Figure 8. 2D Schematic of the DMST model

The DMST model simultaneously solves two equations for the stream-wise force at the actuator disk; one obtained by conservation of momentum and other based on the aerodynamic coefficients of the airfoil (lift and drag) and the local wind velocity. These equations are solved twice; for the upwind and for the downwind part of the rotor.

Upwind half $\pi/2 \le \theta \le 3\pi/2$:

$$w = \sqrt{(u_i \sin(\theta))^2 + (u_i \cos(\theta) + \omega R)^2} \qquad (50)$$

$$\alpha = \tan^{-1}\left(\frac{(1-a)\sin(\theta)}{(1-a)\cos(\theta)+\lambda} \right) \qquad (51)$$

Downwind half $3\pi/2 \le \theta \le \pi/2$:

$$w' = \sqrt{(u_i'\sin(\theta))^2 + (u_i'\cos(\theta)+\omega R)^2} \qquad (52)$$

$$\alpha = \tan^{-1}\left(\frac{(1-a')\sin(\theta)}{(1-a')\cos(\theta)+\lambda} \right) \qquad (53)$$

Once the new relative wind speed and angle of attack are found using the new induction factor; the thrust coefficient, torque coefficient and power coefficient can be calculated easily using Equation (39), (42) and (43).

3. METHODOLOGY

This paper evaluates the performance of fixed pitch vertical axis wind turbine with three blades using DMST model and 2D unsteady flow analysis using CFD. In the analysis, the conventional NACA0012 symmetrical airfoil was used. This airfoil is selected due to the availability of experimental data.

3.1 DMST Analysis

For the VAWT analysis using DMST model, the normal NACA0012 airfoil was set to 0.2m chord length, and the turbine radius was set to 2m. The height of the turbine is taken to be 4m. With the number of blades considered to be 3, the solidity (Bc/D) becomes 1.5. The wind velocity used in the analysis is 5m/s and the tip speed ratios (λ) are 0.25, 0.5, 1, 2, 3, 4, 5 and 6. The total number of stream tube used for the analysis is 12 with $\Delta\theta = 15°$. The iterative procedure used in the DMST model analysis is shown in Figure 9. A spreadsheet is used for easy management of the data. The induction factors a and $a^{'}$ are calculated for upstream of the turbine and the downstream tubes of the turbine respectively. The lift and drag coefficients for NACA0012 section used are the data of Sheldal and Klimas [9]. Since the momentum equation in (12) is not applicable beyond induction factor of 0.5, the Glauert empirical formula is used to calculate the thrust coefficients for $0.4 < a < 1$ and $0.4 < a^{'} < 1$.
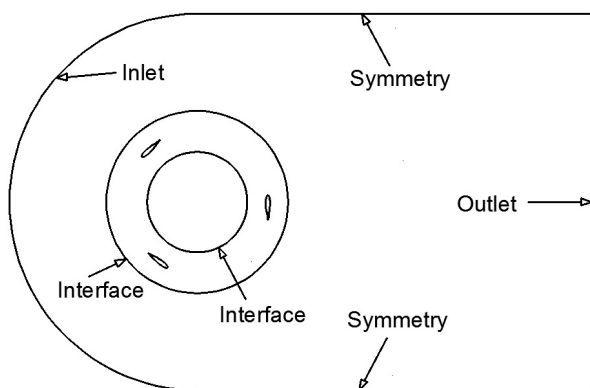
3.2 CFD Analysis

Similarly, for the VAWT analysis using CFD, the same airfoil was set to 0.2 m chord length with radius equal to

2 m. ANSYS software is used to create 2D model of the turbine and the mesh. The model and mesh generated were then read into Fluent for numerical iterate solution. The RANS equations were solved using the green-gauss cell based gradient option and the sliding mesh method was used to rotate the turbine blades. The RNG k-ε model was adapted for the turbulence closure. The boundary conditions are shown in Figure 10. The inlet was defined as a velocity inlet, which has constant inflow velocity, while the outlet was set as a pressure outlet, keeping the pressure constant.
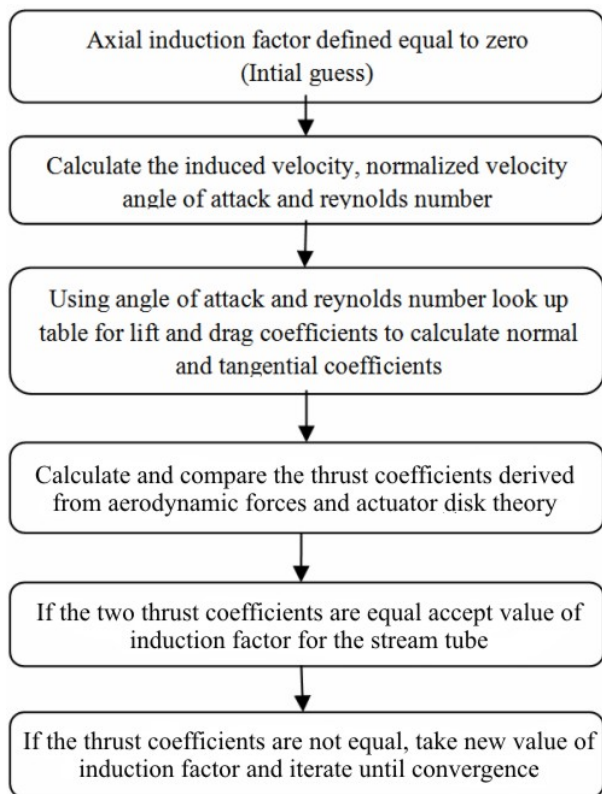
Figure 9. Iterative Procedure used to calculate the flow velocity in DMST model

The mesh generated has a total of 84,839 nodes and 83,641 elements. Complete 2D model mesh and the mesh near the rotor for the numerical analysis are shown in Figure 11 and Figure 12. The no slip boundary condition was applied on the turbine blades, which set the relative velocity of the blades to zero.
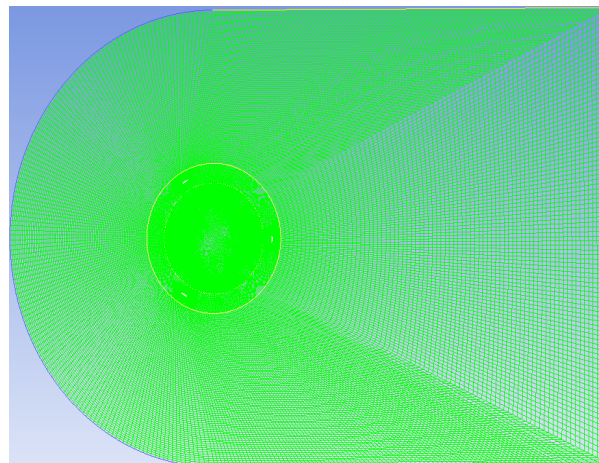

Figure 10. Boundary conditions

For the flow condition in the CFD analysis; a constant inlet wind velocity of 5m/s is used for the tip speed
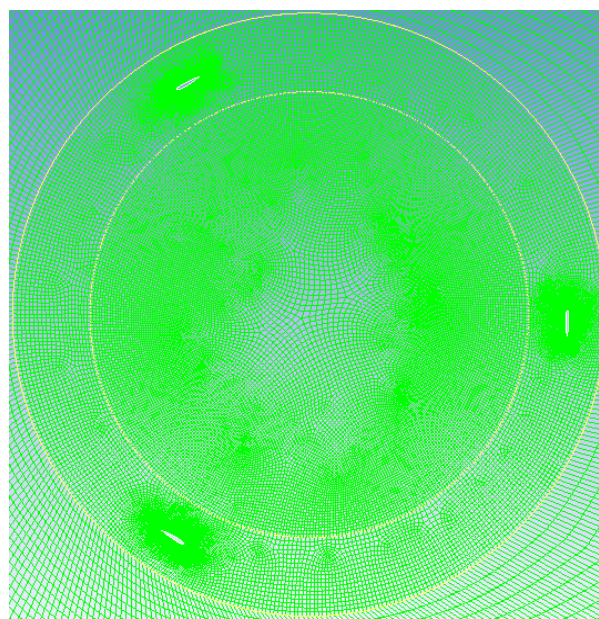
ratios and the corresponding angular velocities shown in Table 1.

Table 1.Flow condition in CFD Analysis

λ	0.25	0.5	1	2	3	4	5	6	7
ω (rad/s)	0.625	1.25	2.5	5	7.5	10	12.5	15	17.5

Figure 11. Mesh of the 2D Model

Figure 12. Mesh near the rotor

4. RESULTS AND DISCUSSIONS

The power coefficient (CP) computed using CFD and DMST models is shown in Figure 13. CP of DMST is found using the iterative procedure shown in Figure 9 where as in the CFD analysis, the CP was obtained from the ratio of the modeled turbine power to the available wind power in the air. The power of the modeled turbine is the result of average torque which is found in the CFD simulation multiplied by angular velocity.

As can be seen, both CFD and DMST model C_P curves show that the turbine generates negative and/or minimum torque for lower tip speed ratios. The DMST model underestimates the C_P value at lower tip speed ratios but it predicts higher C_P value which is 0.41 at a

tip speed ratio of around 4. Figure 13 is in agreement with [10, 11].
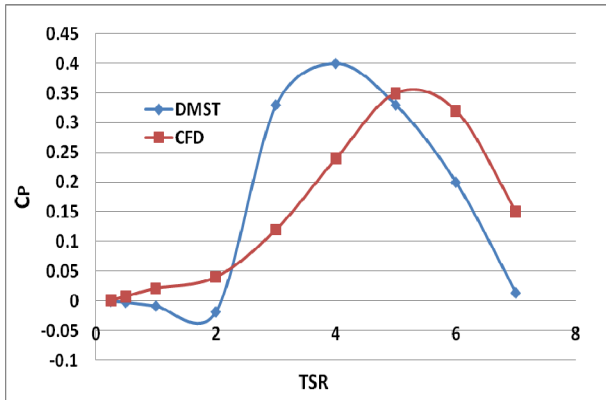

Figure 13. Power coefficient result for DMST and CFD

Figures 14-17 show torque values obtained using DMST model and CFD simulations for NACA0012 blade. Each of them shows the torque values in N-m for complete revolution and tip speed ratios 0.5, 1, 3 and 4. Torque of DMST was found using the iterative procedure shown in Figure 9 where as in the CFD analysis, the torque was obtained from the moment coefficient, density, free stream wind velocity, area and radius of the modelled turbine. As can be seen in the torque graphs there are high fluctuations with each revolution. The average torque values at low tip speed ratios in DMST model are close to zero and increases with increasing TSR.
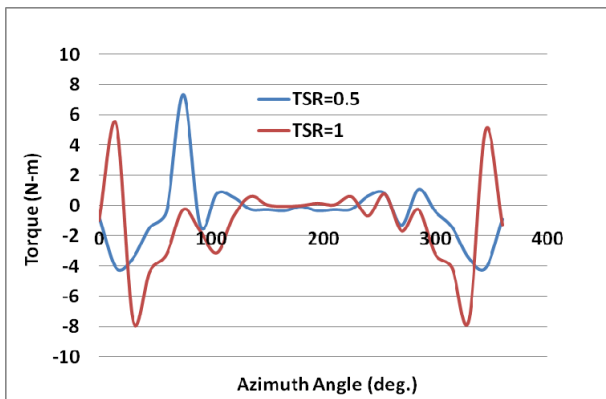

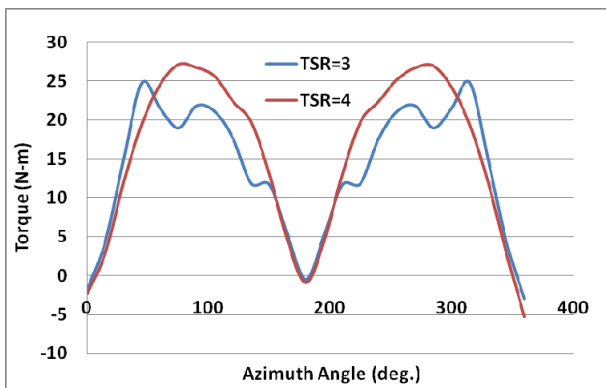**Figure 14. Torque plot using DMST model at TSR=0.5 and 1**

Figure 15. Torque plot using DMST model at TSR=3 and 4

Symmetrical airfoil like NACA0012 is a conventional airfoil section used in Darrieus type VAWTs. However, the main drawback with this type of section is its

minimum or negative torque generation at lower TSRs as can be seen in the above figures. This is the reason for not being able to self start. Some scholars [12-13] have tried to improve self starting of VAWTs.
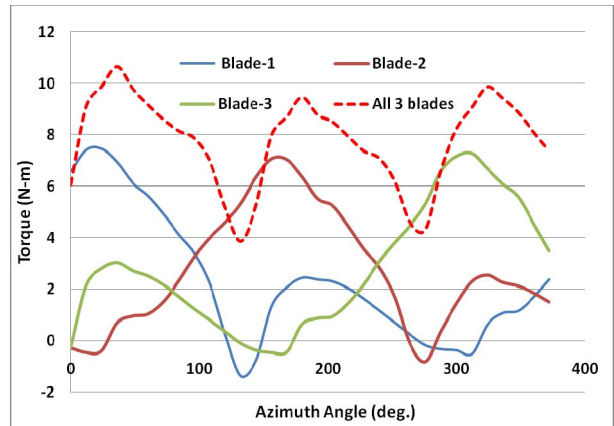

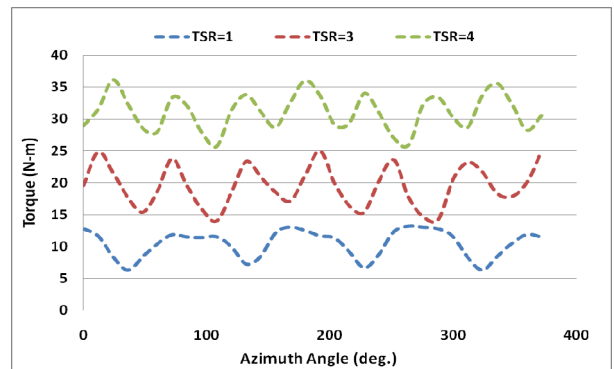**Figure 16. Torque plot using CFD model at TSR=0.5**

Figure 17. Torque plot using CFD model at TSR=1, 3 and 4

The blade aerodynamic forces and torque values are computed from the solution of RANS equations through the integration of the pressure and shear stress over the blade surfaces. CFD can capture flow features such as vortex/blade interaction and vortex shedding into the wake. Figure 18 and 19 shows the absolute velocity contours for tip speed ratio of 4 and eddy distribution of viscous standard k-ε turbulence model. The results are in agreement with Marco Raciti [14] and Huimin Wang [15]. As expected the eddy and velocity in the region of wind turbine's rotation is much larger than the air flow of upstream.
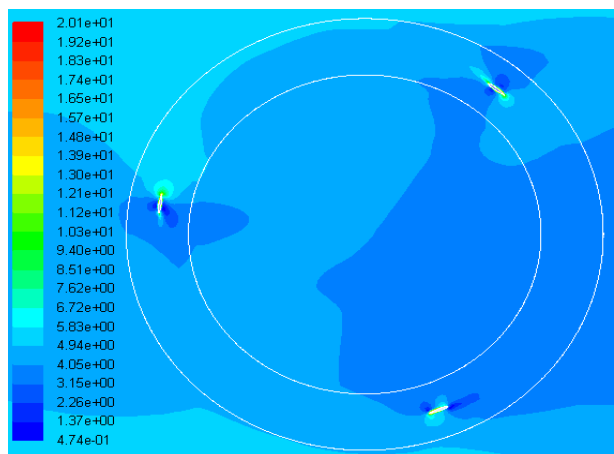

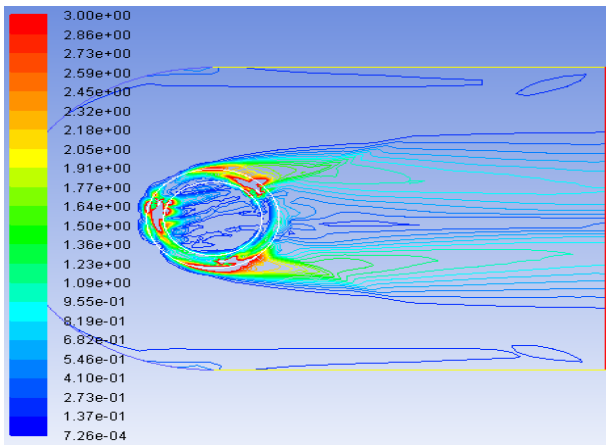**Figure 18. Contours of absolute velocity for TSR=4**

Figure 19. Distribution of eddy for TSR=4

5. CONCLUSION

In this paper, analytical and numerical investigation of performance of Darrius type straight blade VAWT is done using NACA0012 as a blade profile. The analytical investigation is done using DMST model. In the numerical investigation, 2D unsteady flow of VAWT is analyzed using CFD. The C_P value obtained from the DMST model and CFD were then compared. DMST model overestimated the maximum C_P value.

The advantage of CFD is that it provides a platform to explore various airfoil shapes for optimum VAWT performance but it is computationally intensive. As can be seen from the CP and torque curves obtained by CFD and DMST model, negative and/or minimum CP and torque are generated at lower tip speed ratios, which implies that NACA0012 is not self starting. Darrieus type straight blade VAWTs are advantageous in several aspects if its inability to self start is resolved.

REFERENCES

[1] Sathyajith, M.: *Wind Energy Fundamentals, Resource Analysis and Economics*: Springer-Verlag Berlin Heidelberg, Netherlands, 2006.

[2] Claessens, M.C.: *The Design and Testing of Airfoils for Application in Small Vertical Axis Wind turbines*, Delft University, November 2009.

[3] Islam, M., Ting, D.K., and A. Fartaj: Aerodynamic models for Darrieus-type straight-bladed vertical axis wind turbines, Renew and Sustain Energy Reviews, Vol. 12, No. 4, pp. 1087-1109, 2008.

[4] Duncan, W.J.,: *An Elementary Treatise on the Mechanics of Fluids* , Edward Arnold Ltd, 1962

[5] Paraschivoiu, I., Saeed, F. and Desobry, V.: *Prediction capabilities in vertical axis wind turbine aerodynamics*, Berlin, Germany, 2002.

[6] Paraschivoiu, I.: *Double-Multiple Streamtube Model for Darrieus Wind Turbines*, Institute de recherché d'Hydro-Québec, Canada.

[7] Templin, R.: Aerodynamic performance theory for the vertical axis wind turbine, National Research Council Canada, Tech. Rep. LTR-LA-10, 1974.

[8] Strickland, J.: The Darrieus Turbine: A Performance Prediction Model Using Multiple Stream Tubes, Technical Report SAND75-041, Sandia National Laboratories, Albuquerque, 1975.

[9] Sheldal, R.E. and Klimas, P.C.: Aerodynamic Characteristics of Seven Airfoil Sections: Sandia National Laboratories, 1981.

[10] Klimas, P.C. and Sheldahl, R.E.: Four Aerodynamic Prediction Schemes for vertical-Axis wind Turbines: A compendium, Sandia National Laboratories, Springfield, 1978.

[11] McGowan, R., Lozano, R., Raghav, V., and Komerath, N.:Vertical Axis Micro Wind Turbine Design for Low Tip Speed Ratios, Georgia Institute of Technology Atlanta, United States.

[12] Paraschivoiu, I., Trifu, O., and Saeed, F.: H-Darrieus Wind Turbine with Blade Pitch Control, Hindawi Publishing Corporation, Vol. 2009.

[13] Klimas, P.C. and Worstell, M.H.: Effects of Blade Preset Pitch/offset on Curved-Blade Darrieus Vertical Axis Wind Turbine Performance, Sandia National Laboratories, October 1981.

[14] Castelli, M.R.: Effect of Blade Number on a Straight-Bladed Vertical-Axis Darreius Wind Turbine, World Academy of Science, 61, 2012.

[15] Wang, H.: Analysis on the aerodynamic performance of vertical axis wind turbine subjected to the change of wind velocity, Kunming University of Science and Technology, 2011.

NUMENCLATURE

A	Projected frontal area of turbine
a	Induction factor for the upstream tube
a'	Induction factor for the downstream tube
B	Number of blades
c	Blade chord length
C_D	Blade drag coefficient
C_L	Blade lift coefficient
C_n	Normal force coefficient
C_P	Power coefficient
C_Q	Torque coefficient
C_t	Tangential force coefficient
C_T	Thrust coefficient
D	Turbine diameter
F_N	Normal force
F_T	Tangential force
h	Height of turbine
$\dot{m}$	Mass flow rate
N_θ	Number of stream tubes
P	Power by the turbine
p_d	Downwind pressure of the rotor
p_u	Upwind pressure of the rotor
p_o	Pressure of undisturbed air
p'	Pressure drop across rotor plane
Q_i	Instantaneous torque
Q_{avg}	Average torque
R	Turbine radius
T	Thrust force
T_{avg}	Average thrust force
T_i	Instantaneous thrust force
u_∞	Free Stream wind velocity
u_e	Equilibrium value wind velocity
u_i	Induced velocity in the upstream side
u'_i	Induced velocity in the downstream side
u_R	Wind velocity at the rotor
u_w	Wake velocity in upstream side

$u^{'}_{w}$ Wake velocity in downstream side
w Relative velocity in the upstream side
$w^{'}$ Relative velocity in the downstream side

НУМЕРИЧКО И АНАЛИТИЧКО ОДРЕЂИВАЊЕ ПЕРФОРМАНСИ ВЕТРОТУРБИНА СА ВЕРТИКАЛНОМ ОСОМ ОБРТАЊА

Асресс Мулугета Биадго, Александар Симоновић, Драган Комаров, Слободан Ступар

Већина истраживања везаних за ветротурбине су фокусирана на прецизно одређивање њихове ефикасности. У раду је истакнут напредак који је остварен у развоју аеродинамичких модела за анализу ветротурбина са вертикалном осом обртања, са посебним освртом на приступима заснованим на анализи струјања ваздуха кроз струјне цеви. Изведена је нумеричка и аналитичка анализа перформанси за невитоперену NACA0012 лопатицу ветротурбине са вертикалном осом обртања. Нумеричка симулација је урађена за нестационарно, дводимензионо струјање око модела ветротурбине са вертикалном осом обртања помоћу софтвера FLUENT решавањем Рејнолдсових једначина. Напослетку, извршено је поређење резултата добијених применом CFD-а и DMST аналитичког модела. Резултати добијени на ова два начина су указали на постојање минималних или негативних обртних момената и перформанси при ниским коефицијентима рада ротора, што имплицира отежано самопокретање ротора анализиране конфигурације са NACA0012 аеропрофилом.